Research Square

Preprints are preliminary reports that have not undergone peer review.
They should not be considered conclusive, used to inform clinical practice,
or referenced by the media as validated information.

Uncertainty on short-term vertical displacements of a tunnel in soft soil due to spatial variability of undrained elasticity modulus

Marcos Edgardo Delgado-Muñiz

mdelgadom@iingen.unam.mx

Instituto de Ingeniería, UNAM, Universidad Nacional Autónoma de México

Gabriel Auvinet-Guichard

Instituto de Ingeniería, UNAM, Universidad Nacional Autónoma de México

Sergio Felipe Zaldivar-Reyes

Instituto Tecnológico y de Estudios Superiores de Monterrey

Research Article

Keywords: Tunneling, soft soil, soil variability, stochastic finite element method, Monte Carlo simulation

Posted Date: May 20th, 2026

DOI: https://doi.org/10.21203/rs.3.rs-9622205/v1

License: This work is licensed under a Creative Commons Attribution 4.0 International License.
Read Full License

Additional Declarations: No competing interests reported.

Uncertainty on short-term vertical displacements of a tunnel in soft soil due to spatial variability of undrained elasticity modulus

Marcos Edgardo Delgado-Muñiz*
Instituto de Ingeniería, UNAM, Universidad Nacional Autónoma de México, Circuito Escolar s/n, Ciudad Universitaria, Coyoacán, C.P. 04510, Ciudad de México, México, https://orcid.org/0009-0006-1751-6240, e-mail: mdelgadom@iingen.unam.mx

Gabriel Auvinet-Guichard
Instituto de Ingeniería, UNAM, Universidad Nacional Autónoma de México, Circuito Escolar s/n, Ciudad Universitaria, Coyoacán, C.P. 04510, Ciudad de México, México, https://orcid.org/0000-0003-4674-1659

Sergio Felipe Zaldivar-Reyes
Instituto Tecnológico y de Estudios Superiores de Monterrey, Escuela de Ingeniería y Ciencias, Ave. Eugenio Garza Sada 2501, C.P. 64849, Monterrey, Nuevo León, México

Abstract The objective of this paper is to assess the uncertainty on vertical displacements of a tunnel in lacustrine soil in the Valley of Mexico during the excavation process and installation of primary lining, when considering the variability of the undrained elasticity modulus (E_u). The short-term vertical displacement response of the tunnel is simulated using the three-dimensional finite element method. The variability of the undrained elasticity modulus in the first clay layer (FCL) of the soil profile is represented by anisotropic random fields. Stochastic analyses are performed according to two scenarios. First, the vertical unidimensional variability of E_u modulus is represented by a one-dimensional random field. In the second scenario, variability of the modulus in the three directions of the domain is considered. The uncertainty associated to the evaluation of short-term displacements of the tunnel and surrounding soil of the first clay layer is quantified using the Monte Carlo method and the results obtained with both models are compared.

Keywords Tunneling, soft soil, soil variability, stochastic finite element method, Monte Carlo simulation

1 Introduction

Tunnel construction represents a significant geotechnical engineering challenge, particularly in cases where the soil exhibits complex mechanical behavior (Liu et al. 2025). According to Peck (1969), the fundamental requirements for a satisfactory tunnel are as follows: the first one is that the tunnel should be able to be built; the second requirement is that the tunnel should withstand all the influences to which it may be subjected during its lifetime and the third one is that construction of the tunnel should not excessively damage below or above ground structures adjacent to the tunnel (Bobet and Einstein 2023). In soft soils, such as those found in the Valley of Mexico, significant surface displacements occur during the excavation and construction stages of tunnels. These displacements are attributed to three primary effects: 1) the closure of the excavation, 2) the alteration in the tunnel's geometry, and 3) the upward movement of the tunnel due to soil unloading (Bobet and Einstein 2023). This latter effect has been denominated the "bubble effect". This phenomenon is the result of a complex interaction between the unloaded soil and the primary lining (Auvinet and Rodríguez 2011; Zaldivar et al. 2012).

The spatial variability of geological conditions such as soil strength, permeability, and deformation modulus, presents a challenge in geotechnical engineering, as it critically influences the performance, safety, and reliability of geotechnical systems (Baecher 2023; Christian 2004; Feng et al. 2025). The capture and modeling of this variability is crucial to optimize design, minimize risks, and quantify the uncertainty on the mechanical behavior of the geotechnical structures (Huang et al. 2017; Phoon 2023; Li et al. 2024; Feng et al. 2025). The influence of spatial variability of soil parameters in the response of the geotechnical systems is frequently modeled using random field theory. A series of studies have been conducted over the past several decades concerning the impact of soil variability on geotechnical systems employing random fields by researchers such as Vanmarcke (1977), Auvinet and Abaziou (1993), and Phoon and Kulhawy (1999). For several decades, random field analyses have been employed in the study of key topics in geotechnical engineering, including liquefaction (Popescu et al. 1997), bearing capacity (Popescu et al. 2005), settlement of foundations (Griffiths and Fenton 2007), slope stability (El-Ramly et al. 2002) and excavations (Li et al. 2023). In the tunneling area, the effect of soil spatial variability on structural behavior has received attention from Huang et al. (2017), Ali et al. (2017), Gong et al. (2018), Whu et al. (2021), Liu et al. (2025) and Sherhal et al. (2025).

This paper presents a study of the uncertainty in the field of vertical displacements assessed by short-term numerical analyses considering elastic behavior during the excavation process and installation of the primary lining of a tunnel. The study is based on the Mohr Coulomb constitutive model and incorporates soil spatial variability of undrained elastic modulus (E_u). The following is a summary of the analyses presented in this study: i) Deterministic three-dimensional deterministic numerical analysis was performed to assess the mechanical behavior of the tunnel ii) Spatial variability of the undrained modulus of elasticity (E_u) in the FCL was represented by two different random fields (1D and 3D), considering measurements of the first clay layer (FCL) iii) Three-dimensional probabilistic numerical analyses were performed to determine the mechanical behavior of the tunnel, incorporating the variability of the E_u modulus in the FCL and iv) The magnitude and uncertainty of the field of vertical displacements were quantified using the Monte Carlo method by means of the expected value, standard deviation, and coefficient of variation.

Finite element analyses were performed using PLAXIS 3D software. To perform the Monte Carlo simulations, subroutines were developed within a Python programming environment, allowing for the execution of multiple iterations.

2 Random fields

A random field can be conceptualized as a set of random variables distributed in space. A random field $\{V(X), X \in \Omega^p\}$ with dimension p = 1, 2, or 3, represents a set of random variables defined in specific points $X(x,y,z)$ of a certain domain Ω^p (Vanmarke 1984; Auvinet 2002; Hristopulos 2020; Xie et al. 2025). In geotechnical engineering, $V(X)$ is defined as a property of either physical (e.g. water content), mechanical (e.g. undrained shear strength), or geometric type (e.g. thickness of a certain stratum), (Auvinet 2002). Mathematically, the spatial variability of soil properties can generally be modeled as the sum of two components: the deterministic trend $T(X)$ and a residual field $R(X)$, which is generally assumed to be stationary (Vanmarcke 1977; Phoon and Kulhawy 1999). This model is expressed as follows:

$$V(X) = T(X) + R(X) \tag{1}$$

where $V(X)$ is the value of geotechnical property at a given location.

The characteristics of the random field (expected value, variance and autocorrelation functions) are obtained by statistical methods from the available data (boreholes results, correlations with index properties or expert assessments) (Auvinet 2002).

To obtain specific realizations of the random field, several methods can be used such as i) Matrix decomposition (MD) (Alabert 1987; Davies 1987), ii) Discrete Fourier transform method, iii) Fast Fourier transform method (FFT), iv) Turning bands method (TBM) (Chilès and Delfiner 1999) and v) Karhunen-Loève expansion (K-L) (Ghanem and Spanos 1991). Non-Gaussian fields may be transformed and realizations be obtained from the associated Gaussian fields (Penning et al. 2025). In this paper, the matrix decomposition method was adopted.

2.1 Matrix decomposition method (MD)

The possible configurations of the random field can be generated by means of the matrix decomposition (MD) method. The autocorrelation matrix (ρ_E) associated to the coordinates $X_1, X_2, \ldots X_n$ of the nodes of a given mesh (or centers of elements) in the domain presents the following form:

$$\rho_E = \begin{bmatrix} 1 & \rho(X_1 - X_2) & \cdots & \rho(X_1 - X_n) \\ \rho(X_2 - X_1) & 1 & \cdots & \rho(X_2 - X_n) \\ \vdots & \vdots & \ddots & \rho(X_3 - X_n) \\ \rho(X_n - X_1) & \rho(X_n - X_2) & \cdots & 1 \end{bmatrix} \tag{2}$$

In the case of a 3D random field, the correlation structure was considered to be a squared exponential correlation function (Auvinet 2002; Fenton and Griffiths 2008; Zhou et al. 2022):

$$\rho = exp\left(-\sqrt{\left(\frac{\tau_x}{\delta_x}\right)^2 + \left(\frac{\tau_y}{\delta_y}\right)^2 + \left(\frac{\tau_z}{\delta_z}\right)^2} \right) \tag{3}$$

where δ_x, δ_y, δ_z are the correlation distances in the horizontal (x, y) and vertical (z) directions, τ_x, τ_y, τ_z are the distances between the coordinates of pairs of points.

The autocorrelation matrix ρ_E is decomposed into the product of a lower triangular matrix L and the transpose matrix (L^T) by means of the Cholesky matrix decomposition as follows:

$$L \cdot L^T = \rho_E \tag{4}$$

Given the matrix L, it is possible to obtain the values of a normalized gaussian random field G, based on the following expression:

$$G = L \cdot Z \tag{5}$$

where Z is a sequence of independent normal random variables. The normalized random field G can be transformed into values of the original field of the soil parameter.

The simulation technique MD can be applied to different dimensions of the study domain (Ω^p, p=1, 2 or 3). The prediction of the possible configuration of the random variable can be simulated at a point, node, element, or unit level, depending on the type of problem and the variability conditions of the parameter under consideration. Zhou et al. (2022). The dimensions of the soil units within the domain are defined considering the autocorrelation distance or scale of fluctuation (SOF) of the parameters to be incorporated into the numerical analysis (Huang and Griffiths 2015; Crisp 2020; Crisp et al. 2022). Recommendations found in the literature are summarized in Table 1.

Table 1 Recommendation of soil element sizes as percentage of scale of fluctuation (Crisp et al. 2022)

Model type	Range of variaton (perentege of scale of fluctation, % SOF)	Upper limit (percentage of scale of fluctuation, % SOF)
Elastic	20-25	50
Plastic	2-5	50 (or lower)

3 Stochastic Finite Element Method (SFEM)

The stochastic finite element method (SFEM) is an extension of the deterministic finite element method (FEM). It is a convenient way to describe and quantify the propagation of uncertainty in geotechnical systems. This is possible by considering the variability in the input parameters in the time and/or spatial domain. The expression (6) denoting the system of equations of the stochastic finite element method is obtained by incorporating random variables/fields into the system of equations of the classical finite element method (Stefanou 2009; Papadopoulos and Giovanis 2018; Zheng et al. 2023).

$$\mathbf{K}(\theta)\mathbf{u}(\theta) = \mathbf{F}(\theta) \tag{6}$$

where $\mathbf{K}(\theta) \in \Omega^{n \times n}$ is the stochastic global stiffness matrix representing stochastic properties of the physical model under investigation, n is the number of degrees of freedom, $\mathbf{u}(\theta) \in \Omega^n$ is the unknown stochastic displacement and $\mathbf{F}(\theta) \in \Omega^n$ is the stochastic force vector associated with source terms (Zheng et al. 2023).

In general, the task of computing the high-precision solution of Eq. (6) presents a considerable challenge. There are three primary variants of SFEM: (i) the perturbation approach, which is based on a Taylor series expansion of the response vector (Auvinet et al. 1996); (ii) the spectral stochastic finite element method, where each response quantity is represented using a series of random Hermite polynomials (Ghanem and Spanos 1991); and (iii) Monte Carlo simulation (Stefanou 2009; Papadopoulos and Giovanis 2018). In this paper, the SFEM is employed through the utilization of the Monte Carlo simulation approach.

3.1 Monte Carlo simulation

Monte Carlo Simulation (MCS) is the most general and direct approach for the solution of the equation (6) of the Stochastic Finite Element Method. The following eight steps are fundamental to this approach: i) identification and acknowledgment of the factors that introduce uncertainty into the system, ii) selection of random variables to be studied, iii) analysis of the probability distributions of these random variables and their correlation, iv) generation of a set of random fields, v) construction of deterministic finite element model variants in accordance with the generated fields, vi) definition of the number of simulations to be performed, (vii) calculation of model responses for a defined number of simulations, and (viii) statistical analysis of the responses of the system. According to this approach, N_S samples of the stochastic stiffness matrix $\mathbf{K}(\theta)$ is generated, and the deterministic problem of Eq. (6) is solved N_S

times, generating a population for the response vector $\{\mathbf{u}_j\}$ with $j = 1,..., N_S$. The expected value ($E\{u_i\}$), variance (σ^2) and coefficient of variation (CV) of displacements can be estimated using the following expressions:

$$E\{u_i\} \approx \frac{1}{N_S} \sum_{j=1}^{N_S} u_i(j) \tag{7}$$

$$\sigma^2 \approx \frac{1}{N_S - 1} \sum_{j=1}^{N_S} [u_i(j)^2 - N_S(E\{u_i\}^2)] \tag{8}$$

$$CV \approx \frac{E\{u_i\}}{\sigma} \tag{9}$$

4 Methodology

The methodology for the stochastic analysis of the mechanical behavior of geotechnical systems considering variability is summarized in Figure 1. The geotechnical parameter considered as a random field, generally a variable of the constitutive model used in the numerical analysis, is initially selected. A preliminary exploratory analysis of the available experimental geotechnical parameter measurements obtained from either the field or the laboratory. is conducted. A statistical analysis is then used to determine the parameter's expected value and range of variation. This analysis also serves to detect any outliers that may affect subsequent stages. A trend analysis is then performed, and the experimental field is transformed into a stationary residual field (without trend). A structural analysis of the data from the stationary residual field is carried out to obtain correlation distances in preferred directions based on the dimensions and conditions of isotropy or anisotropy of the study domain. Simulation techniques can be used to generate possible values of the geotechnical parameter in each soil unit of the study domain.

The mechanical behavior of the geotechnical system is assessed using both deterministic (FE model) and probabilistic (SFE model) approaches. For the deterministic approach, a geotechnical model is generated with information of thicknesses, constitutive models, and average parameter values for the different layers. Subsequently, the geometry, loads, and properties of the structural elements of the geotechnical system are defined. As a result, a single response the geotechnical system is obtained.

In the stochastic approach, the domain or subdomain of interest is divided into soil units where simulated values of the parameter are incorporated. Multiple responses are generated for the different sets of parameter values. The number of required simulations is defined through a convergence analysis. Uncertainty associated with the variability of the geotechnical parameter can be quantified.

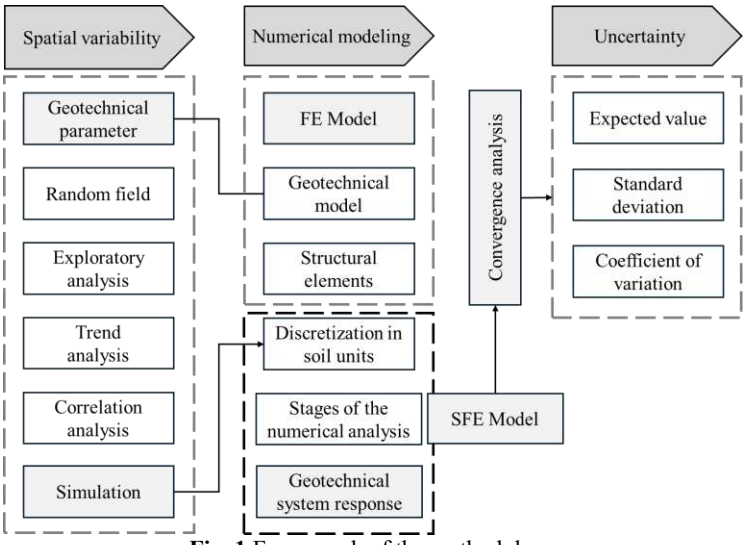


Fig. 1 Framework of the methodology

5 Case study

The site is located in the municipality of Chimalhuacán in the eastern part of the State of Mexico. The geotechnical zoning of Mexico City, in accordance with complementary technical standards for foundation design, designates the

tunnel axis as part of Zone III, also referred to as the lake zone. As illustrated in Figure 2a, eight mixed boreholes were available along the tunnel axis. The maximum exploration depth is approximately 60 m, thereby covering the entire stratigraphic profile of the subsoil.

Figure 2b illustrates the variation of the water content (w) with depth in the study area. The distribution of w is indicative of the presence of five distinct layers. At the top of the profile is the Dry Crust (DC), a thin layer with low water content values (0%-30%). A thicker layer, exhibiting water content values ranging from 100% to 400%, is also observed below the depth of the DC. This layer is composed of highly compressible clay material, identified as the First Clay Layer (FCL). The FCL has an approximate thickness of 35 m. The excavation and placement of the tunnel lining will be carried out from a depth of 13.7 m down to 19.8 m within the FCL. A hard layer (HL) is present below the FCL, consisting of a sandy clayey material with water content values below 50%. A significant increase in water content values ranging from 100% to 300% is evident in a clay stratum with a thickness of 5 meters below the HL. This layer corresponds to the Second Clay Formation (SCL). At the lowest point of the profile, the so-called Deep Deposits (DD) are found. These deposits are composed of rigid materials, such as basalt.

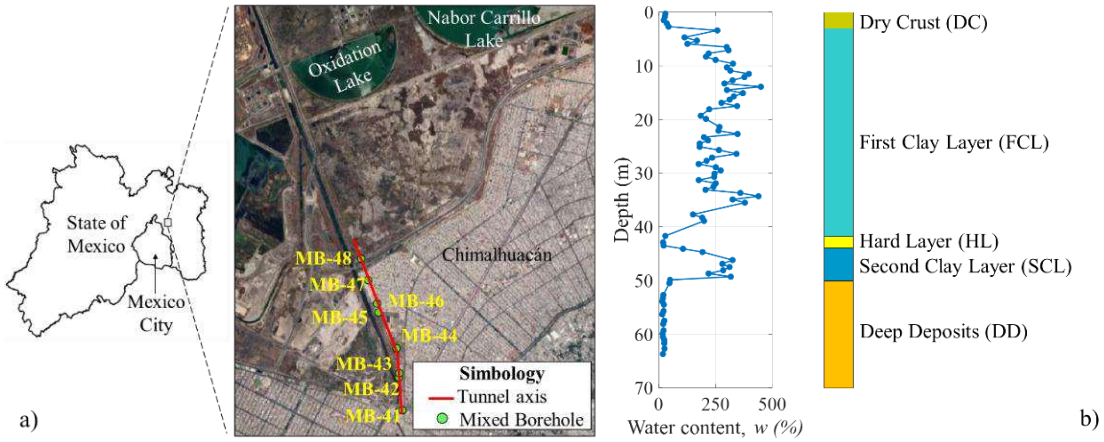


Fig. 2 Location of the study area, a) boreholes distribution and tunnel axis and b) typical water content profile in the study area

5.1 Random field of modulus E_u

Undrained elasticity modulus is considered as a random field E_u(X) distributed within Ω^3. The E_u dataset from the unconsolidated undrained (*UU*) triaxial tests constitutes a sample from that random field. The variability of the E_u modulus in the stochastic analysis was considered only within the First Clay Layer; therefore, only measured values within the depth range of 2 m to 37.5 m were used. The distribution of the 33 E_u values of the experimental field is illustrated in the profile of Figure 4a. A general tendency of modulus to increase in magnitude with depth was observed, with the highest values found at a depth of 18 m and the lowest values occurring in the strata near the borders of the DC and HD.

5.1.1 Exploratory and trend analysis

In this stage, an exploratory analysis of the experimental data of the E_u modulus was carried out. The statistical parameters of E_u are presented in Table 2. The undrained modulus exhibited a range from 1.60 to 5.20 MPa, with a mean value of 3.18 MPa. The values in Table 2 are consistent with the clay layers parameters of the Valley of Mexico clay as reported by Auvinet et al. (2017), and Auvinet (2019). A thorough statistical analysis was conducted, and no atypical values (*outliers*) were identified that would have affected subsequent stages of the process.

Table 2 Statistical parameters of undrained elasticity modulus

Parameter	Value	Unit
Mean	3.18	MPa
Median	3.03	MPa
Mode	2.50	MPa
Standard deviation	1.09	MPa
Maximum value	1.67	MPa
Minimum value	5.17	MPa

The trend of the random field within the study domain Ω^3 was represented by a hyperplane defined by linear regression equation $T(X)=ax+by+cz+d$, where a, b, c, and d, are regression coefficients (Auvinet 2002). The values of these coefficients are shown in Table 3.

Table 3 Linear regression coefficients of E_u

Parameter	Coefficient			
	a	*b*	*c*	*d*
E_u modulus	0.08	-0.12	15.48	213015.87

Removing the trend from the experimental field (Fig 3a), a residual stationary field with zero mean was obtained (Fig 3b).

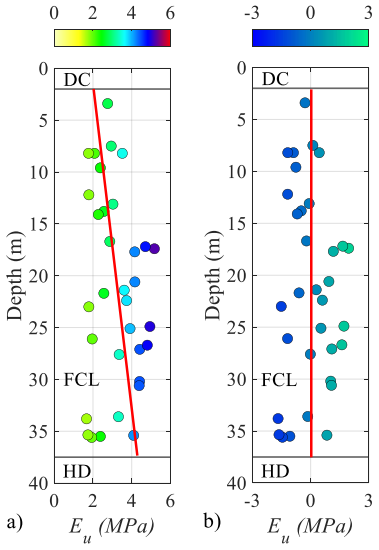


Fig. 3 Profiles of undrained modulus elasticity in the Fist Clay Layer, a) experimental field of E_u and b) residual field of E_u

5.1.2 Correlation analysis

Correlograms were defined in horizontal and vertical directions. The values of the E_u residual field were fitted to a simple exponential correlation model. The correlation distances are indicated in Table 4

Table 4 Correlation distances of the E_u modulus

Directional correlogram	Value	Unit
Vertical	5.0	m
Horizontal	700.0	m

The undrained modulus E_u in the FCL exhibits significantly greater variability along the vertical direction (depth) compared to the horizontal directions. This phenomenon is attributable to the process of formation by horizontal layers of the lacustrine soft soils in Mexico Valley. Figure 4 presents the directional residual correlograms of the E_u modulus.

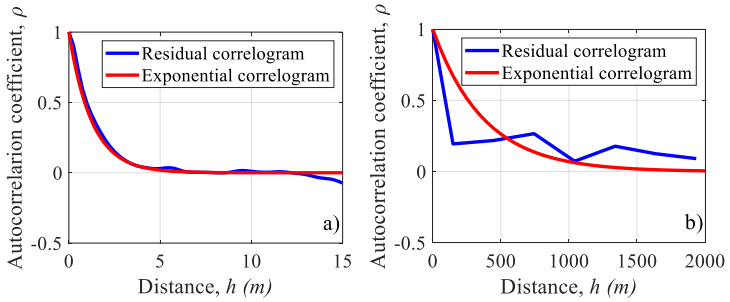


Fig. 4 Directional correlograms of E_u modulus, a) vertical correlogram and b) horizontal correlogram

5.1.3 Conditional simulation

The conditional simulation (matrix decomposition technique) was applied to obtain possible values of E_u in soil units of the first clay layer. In accordance with the criteria outlined above, the FCL was discretized into soil units with variable dimensions, with a maximum value equivalent to 20% of the autocorrelation distance of the undrained modulus of elasticity. In the first scenario the vertical 1D variability of E_u modulus was considered, the domain of the FCL was discretized into 36 soil units with a thickness of 1.0 m (Fig. 5a). In the second scenario (Fig. 5b), the three-dimensional variability of the E_u modulus was considered and the FCL domain was discretized into 483 elements, with thicknesses of 0.5 m, 1.0 m, 1.5 m and 2 m in the vertical direction.

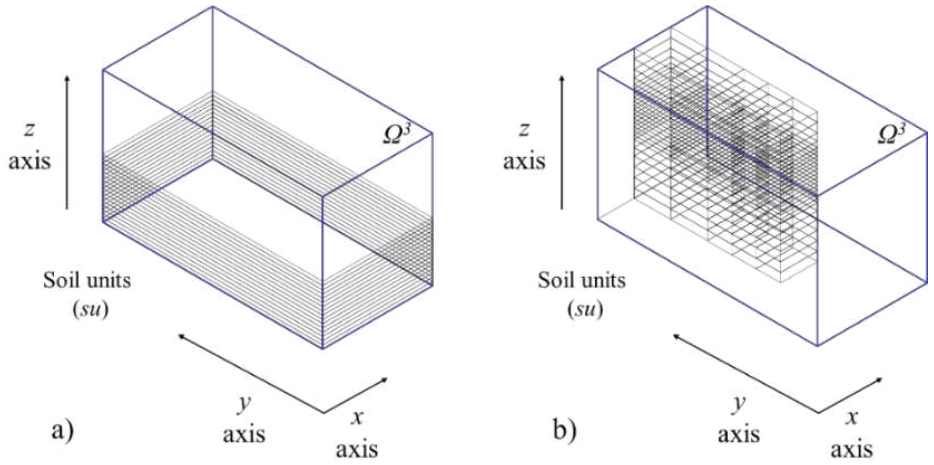


Fig. 5 Discretization of the first clay layer in soil units, a) vertical variability of E_u and b) three-dimensional variability of E_u

Figure 6 presents the results of the conditional simulations of E_u for the two variability conditions assessed. Figure 6a shows the set of simulated profiles for each of the 36 soil units, considering the vertical 1D variability of the E_u modulus. The simulations and the E_u measurements generally exhibit an increase with depth. Additionally, Figure 6b displays four volumes with 3D variability of E_u modulus in the FCL. The 3D distribution of E_u in the volumes indicates a greater degree of variability in the soil units in the vertical direction compared to the horizontal direction. Under both variability conditions, the simulated values of the E_u modulus were found to fluctuate within the range of 1.50 to 5.5 MPa.

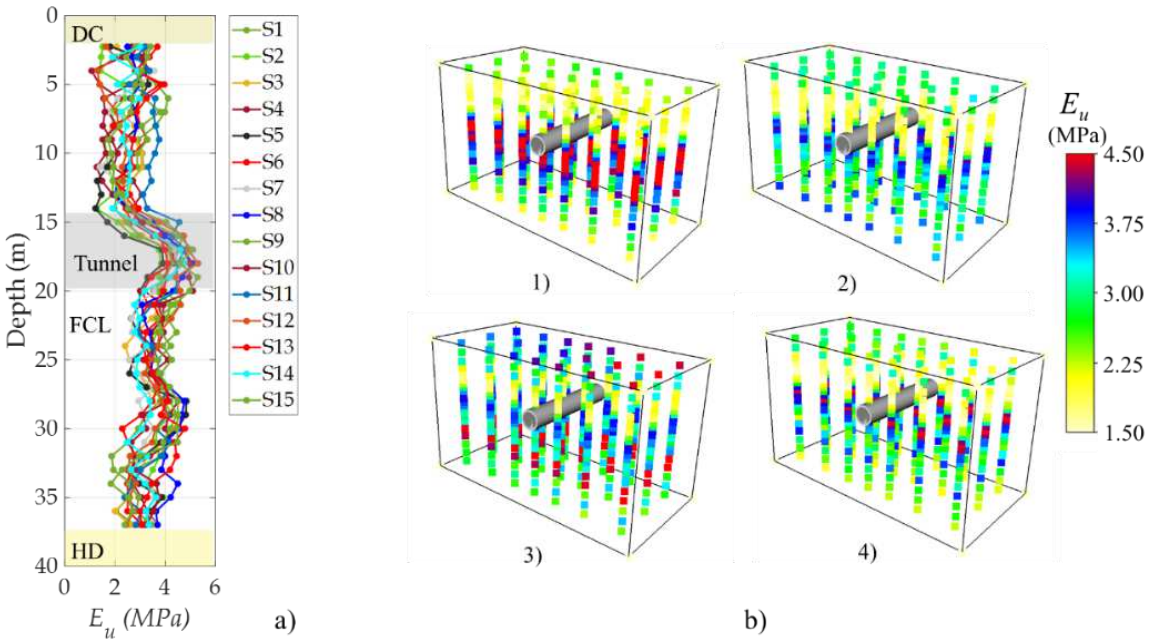


Fig. 6 Conditional simulations of E_u in the Fist Clay Layer, a) vertical variability of E_u and b) 3D variability of E_u

5.2 Numerical analysis of the tunnel behavior

Numerical analysis using the Finite Element Method (FEM) applied to the study of the behavior of geotechnical structures in the Valley of Mexico has been well documented by various authors, including Auvinet and Rodriguez (2011). These authors established considerations based on the type of analysis, the constitutive model, and the application of the FEM. As illustrated in Table 5.

Table 5 Summary of types of numerical analysis in the soft soil of Mexico Valley (Auvinet and Rodriguez 2011)

Analysis type	Soil parameters	Initial condition	Constitutive model	Application
Total stresses	Undrained (E_u, v_u, c_u)	-	Mohr-Coulomb	Immediate settlements
Effective stresses	Drained (E', v')	Drained (no pore pressure generation)	Mohr-Coulomb Soft-soil Cam-Clay-Modified Hardening-Soil	Deferred settlements

The tunnel short term behavior analysis is consistent with the implementation of immediate settlements, as the objective was to calculate the vertical displacements (bubble effect) that occur during the excavation process and installation of the primary lining. In accordance with the criteria of Auvinet and Rodriguez (2011), the short-term numerical analysis of the tunnel was performed in terms of total stresses and the Mohr-Coulomb constitutive model.

Figure 7a illustrates the stratigraphic conditions of the study area considered in the numerical analysis of the behavior of the tunnel. The model presents the following dimensions: 60 m in length, 30 m in width, and 60 m in depth. The stratigraphic configuration of the soil was constituted by the following soil layers: the dry crust (DC), the first clay layer (FCL), the hard layer (HD), the second clay layer (SCL), and the deep deposits (DD). In Figure 7b, the primary lining of the tunnel is also displayed. The center of this lining is situated at a depth of 16.75 m within the first clay layer. The external diameter of the tunnel lining is 6.10 m, while its internal diameter is 5.60 m. The primary lining consists of a series of concrete segments, with a thickness of 0.25 m.

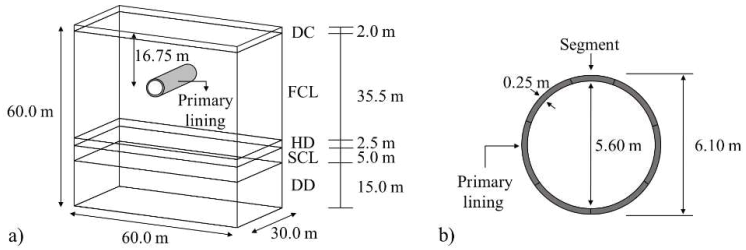


Fig. 7 Soil and tunnel conditions for the analysis, a) stratigraphic conditions of the study area, b) geometry of tunnel lining

The response was evaluated for different widths of the model, expressed as a number of external diameters (D_{ext}) of the primary lining in the horizontal direction: $6D_{ext}$, $10D_{ext}$, $16D_{ext}$, and $20D_{ext}$. It was found that a stable response was obtained for an horizontal dimension larger than $10D_{ext}$.

Table 6 presents the geotechnical model adopted for the numerical analysis. The indicated values were determined from laboratory tests performed on undisturbed samples obtained from the eight mixed boreholes distributed along the tunnel axis. In the case of stochastic analyses, all parameters in Table 6 were considered constant for the different layers, except for the E_u values in the FCL.

Table 6 Geotechnical model for numerical analysis of mechanical behavior of tunnel (short-term)

Layer	Thickness (m)	Unit weight γ, (kN/m^3)	Undrained elastic modulus E_u, (MPa)	Void ratio e, (-)	Poisson's ratio v_u, (-)	Cohesion c_u, (kPa)	Friction angle φ, (º)	Coefficient K_0, (-)
DC	2.0	13.0	5.0	4.0	0.39	30.0	2	0.49
FCL_1	11.0	11.6	2.2	7.7	0.49	22.5	1	0.69
FCL_2	10.0	11.5	4.7	7.8	0.49	19.5	1	0.69
FCL_3	14.5	11.4	2.3	5.9	0.49	26.5	1	0.69
HD	2.5	14.7	10.0	1.8	0.43	15.0	20	0.61
SCL	5.0	12.2	3.8	3.8	0.40	38.5	1	0.58
DD	15.0	15.2	10.0	5.0	0.35	20.0	17	0.24

The primary lining parameters employed in the tunnel behavior analysis are detailed in Table 7. The lining was modeled as a volume element with linear-elastic behavior. To consider the effect of the joints between the ring segments, a value of 0.2 was used for the stiffness reduction factor (α), as proposed by Rodríguez et al. (2024).

Table 7 Parameters of the primary lining of tunnel

Parameter	Thickness (m)	Elasticity modulus, E (GPa)	Compresive strength $f'c$(MPa)	Unit weight, γ (kN/m^3)	Poisson's ratio, v (-)	Stiffness´s reduction factor, α, (-)
Value	0.25	5.20	35.00	24.00	0.16	0.20

The geometric models of the tunnel with the different discretizations of the first clay layer employed in the numerical analysis using the finite element method are illustrated in Figure 8. In deterministic analysis, the FCL was divided into three sublayers (FCL_1, FCL_2, and FCL_3) based on the "classic" criteria, where an average value is assigned to layers of great thickness (Fig. 8a). In the stochastic analysis, the FCL was discretized into 36 soil units (Fig. 8b). Figure 8c illustrates the discretization of the FCL into 483 soil units to consider the 3D variability of the E_u modulus. In this scenario, the units with the lowest thickness are in the tunnel area, which is where the excavation takes place and where the maximum vertical displacements are expected to occur.

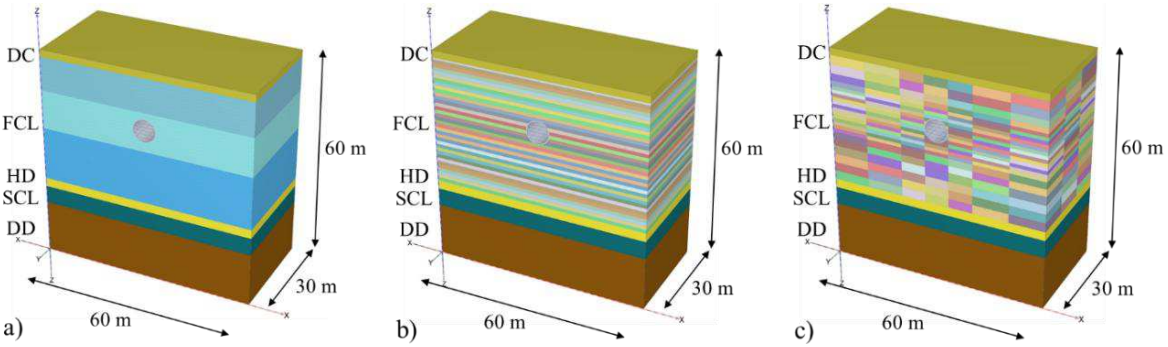


Fig. 8 Stratigraphic discretization of the 3D numerical model of the tunnel, a) deterministic model, b) stochastic model (36 soil units in FLC) and c) stochastic model (483 soil units in FLC)

The mesh where the vertical variability of E_u (36 soil units in FCL) was considered was made up of a total of 170,400 elements (Fig 9a). The mesh where the 3D variability of the E_u module (483 soil units in FCL) was considered was made up of a total of 176,192 elements (Fig 9b). Regarding the boundary conditions, the models were fixed in the x and y directions.

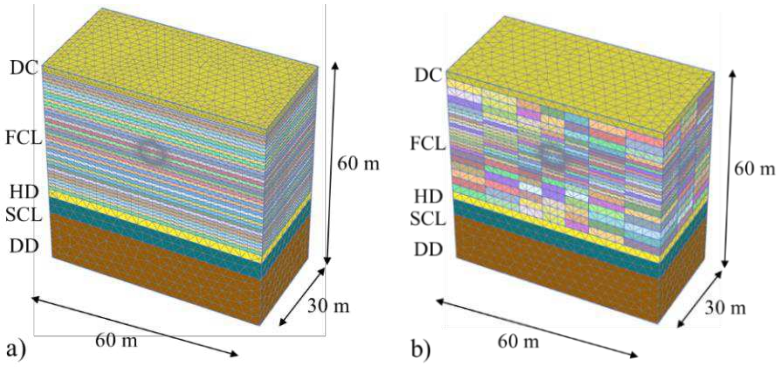


Fig. 9 Finite element mesh of the tunnel model, a) 36 soil units in FLC and b) 483 soil units in FLC

The excavation process was simulated in two stages. In the initial stage, the initial stresses were generated in the medium using the K_0 procedure, at this stage it was not necessary to define the initial pore pressure conditions, because the analysis was performed in terms of total stresses. The second stage was the simulation of excavation and the installation of primary lining. The stages described above were used in both deterministic and stochastic numerical analysis.

5.2.1 Deterministic analysis

Figure 10 shows the results of the vertical displacement field from the deterministic numerical analysis of the mechanical behavior of the tunnel performed using the finite element method (FEM). The configuration of the vertical displacements corresponds to the excavation and installation of the primary lining stage. This approach employs the tunnel model meshes generated in the FCL using the same discretizations as in the stochastic analysis. Figure 10a presents the results obtained from the mesh generated when accounting for 1D variability in the vertical direction of the E_u modulus in the initial clay layer (36 soil units in the FLC), while Figure 10b illustrates the results derived from the mesh when considering the three-dimensional variability of E_u.

In the two deterministic models, the distribution of the vertical displacement field is the same, at the bottom of the tunnel (basin), the maximum vertical displacement in the upward direction present a magnitude of 0.055 m. This displacement is known as the "bubble effect" and is a particular phenomenon that occurs during the construction of tunnels in soft soils. In contrast, at the boundaries of the model, downward movements with a maximum value of 0.012 m were generated. These downward movements were to be expected since short term deformations of the material of the clay layer (FLC) occur at constant volume.

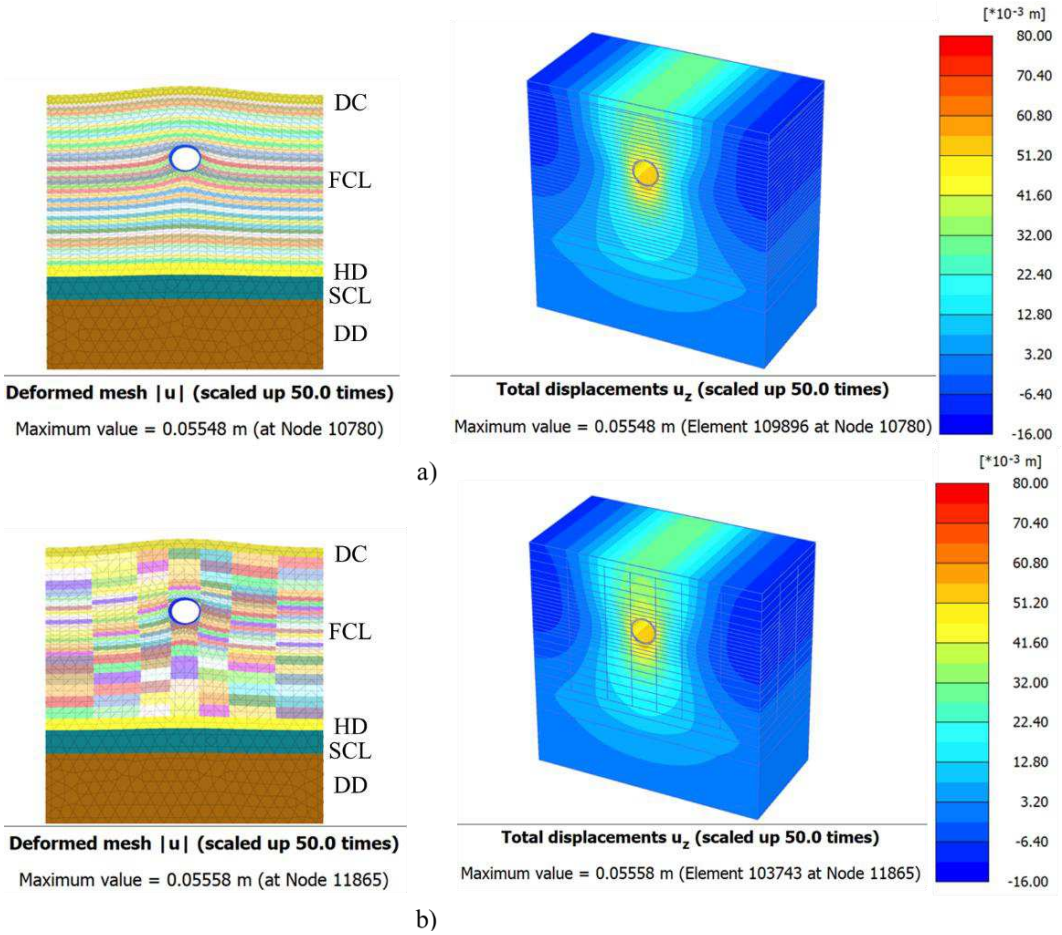


Fig. 10 Deformed mesh and vertical displacements of the deterministic analysis, a) 36 soil units in the FCL and b) 483 soil units in the FCL

Figure 11 presents the cross-sections with vertical displacements situated in the central region of the 3D model of the tunnel. In both sections, the same Gaussian-like bell-shaped distribution and the same displacement values are obtained in the following three areas: i) on the surface (z=0 m), where a maximum displacement of 0.03 m is generated in the central part of the tunnel; in the crown area of the tunnel (z=13.7 m), where a maximum displacement of 0.04 m is observed; and in the basin area of the tunnel (z=19.8 m), where a value of 0.055 m is reached.

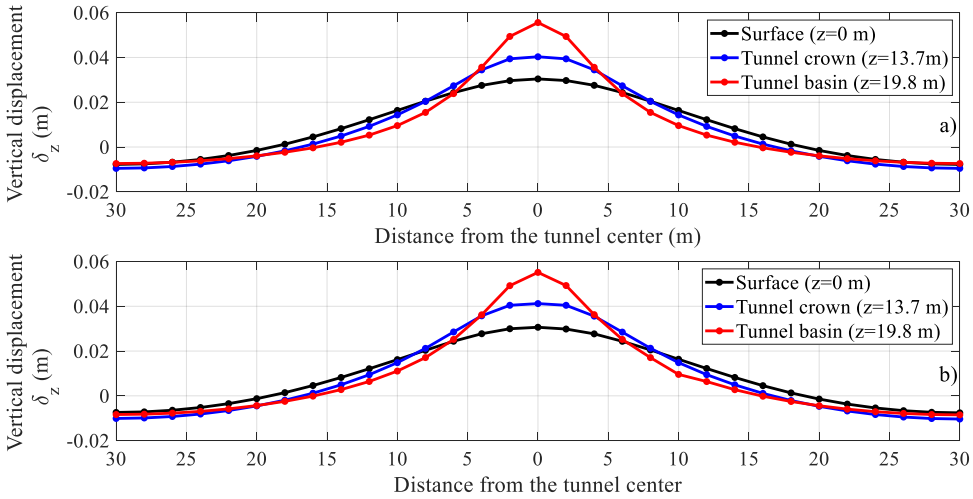


Fig. 11 Cross sections of vertical displacements from deterministic analysis, a) 36 soil units in the FCL and b) 483 soil units in the FCL

5.2.2 Stochastic analysis

As delineated in the methodology, the stochastic analysis incorporates the variability of soil parameters into the numerical analysis using the finite element method (FEM). A thousand conditional simulations of E_u were performed for each variability scenario, resulting in a total of 2,000 realizations being stored. The essence of each of these realizations is a different configuration of the E_u parameter in the first clay formation, leading to different responses of the tunnel. Figure 12 show cross sections in the center of the 3D model with different configurations of vertical displacements during the excavation process and the installation of the primary lining, considering the vertical (Fig. 12a) and 3D (Fig. 12b) variability of E_u modulus. The responses obtained from the numerical simulations are unique, but they follow the same trend observed in the deterministic analysis, with the largest upward magnitudes being found in the tunnel basin area.

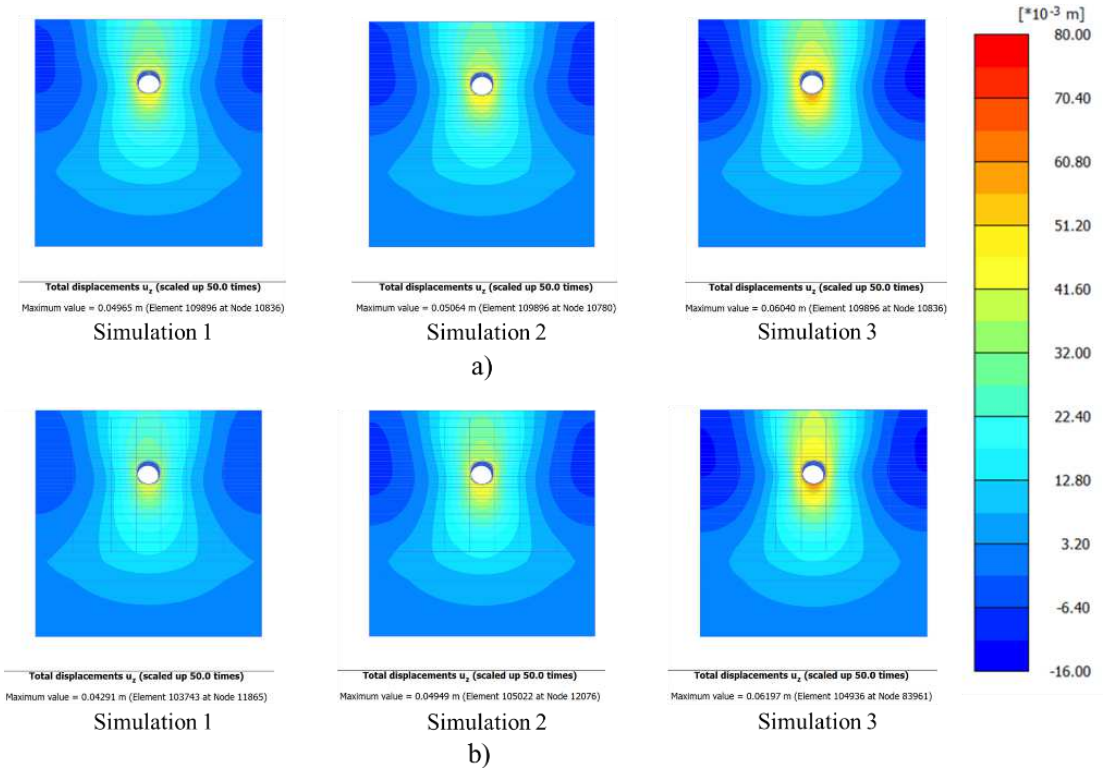


Fig. 12 Cross sections of the vertical displacements field from the stochastic analysis, a) vertical displacements (36 soil units in FLC) and b) vertical displacements (483 soil units in FCL)

Convergence analysis of the Monte Carlo simulation in the stochastic model of tunnel behavior was performed by evaluating the maximum vertical displacement (bubble effect) as the response variable of the system.

Maximum vertical displacement

Figure 13 presents the scatter plots of the maximum vertical displacements. Figure 13a corresponds to the scenario considering the vertical variability of E_u, where a variation in displacements from 0.040 m to 0.074 m was observed. In contrast, Figure 13b illustrates the dispersion of displacements when considering the three-dimensional variability of the E_u modulus. In this scenario, the displacements range from 0.043 m to 0.065 m. The scatter plot values show a greater range of maximum displacement values when considering the vertical 1D variability of E_u.

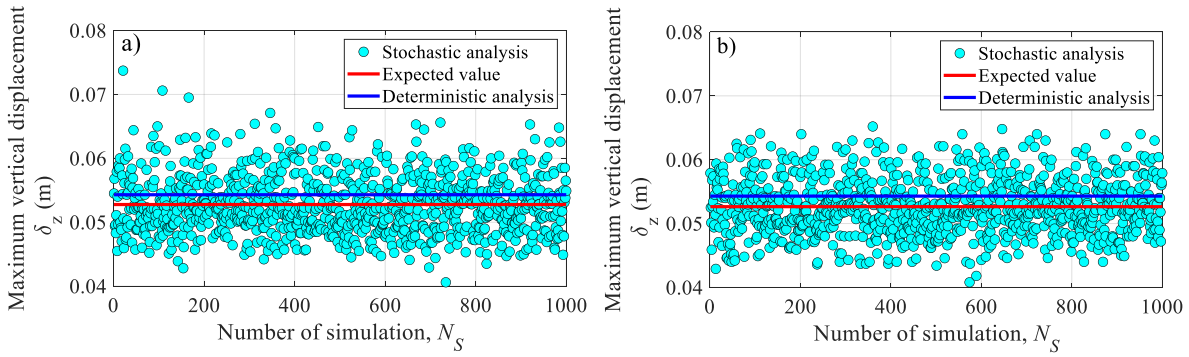


Fig. 13 Dispersion plots of the maximum vertical displacement of the tunnel (1,000 simulations) a) 1D vertical variability of E_u and b) 3D variability of E_u

The convergence of the Monte Carlo simulation technique is presented in the graphs of Figure 14. In Figure 14a, where the 1D vertical variability of E_u was incorporated, the effect of dispersion on the displacement values is shown. The model stabilizes and reaches convergence beyond simulation 600. Figure 14b illustrates the case in which the 3D variability of the E_u modulus was considered. Stability is reached with a smaller number of simulations. In both cases, the expected value of the maximum vertical displacement was 0.0526 m.

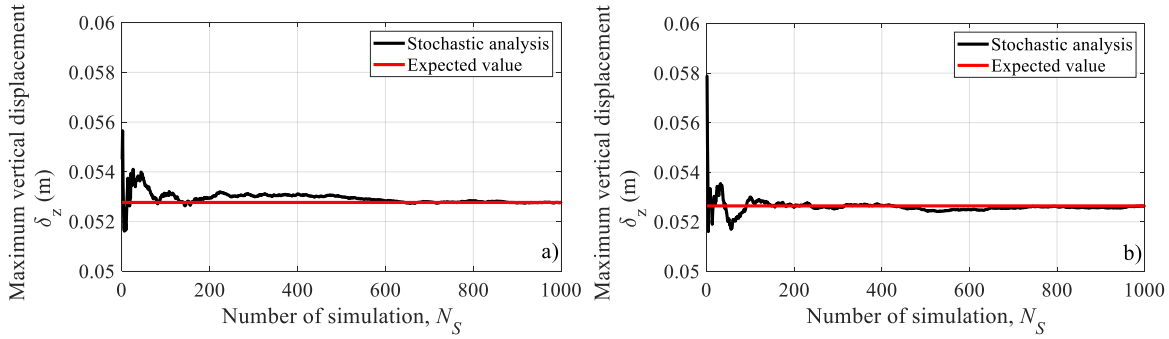


Fig. 14 Convergence plots of the maximum vertical displacement of the tunnel obtained from the stochastic analysis (1,000 simulations), a) vertical variability of E_u and b) 3D variability of E_u

In both scenarios where the variability of the E_u modulus was considered, the maximum vertical displacement of the deterministic analysis exceeds the expected value of the maximum displacements obtained in the stochastic analysis. Table 7 show the statistical summary of the maximum displacements generated in the tunnel basin region for the two variability conditions of the E_u module evaluated.

Table 7 Summary of the statistical parameters of the maximum vertical displacement of the tunnel (1,000 simulations)

Parameter	36 Soil units	483 soil units	Unit
Mean	0.0526	0.0526	m
Median	0.0522	0.0523	m
Mode	0.0543	0.0540	m
Standard deviation	0.0046	0.0043	m
Minimum value	0.0406	0.0429	m
Maximum value	0.0737	0.0652	m

Figure 15 presents the probability density function plots (PDF) for the maximum tunnel displacements. The results of the analyses show a good fit with a normal distribution for the tunnel displacement results. However, the displacements fit is better when the 3D variability of the E_u modulus (Fig. 15b) is considered in the numerical analysis of the tunnel.

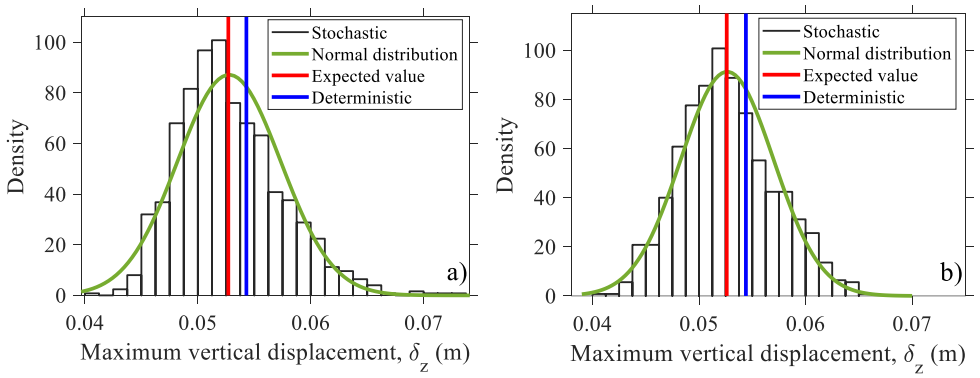


Fig. 15 Probability densities functions (PDF) of the maximum vertical displacement of the tunnel (1,000 simulations) a) PDF of maximum displacements with 1D vertical variability of E_u and b) PDF of maximum displacements with 3D variability of E_u

The quantification of the uncertainty in the field of the vertical displacements of the tunnel associated with the variability of the E_u modulus was performed obtaining the following parameters: i) expected value ii) standard deviation and iii) coefficient of variation.

Expected value

Figure 16 shows the cross-sections of the central part of the 3D model with the expected value of the vertical displacements of tunnel obtained from 1,000 simulations. The cross-sections were defined within the same variation range (0.010 m to 0.050 m) and both exhibit the same distribution of vertical displacements, both upward (heave) and downward (settlement). In the cross-sections (Fig. 16a and Fig. 16b) the maximum displacements of 0.050 m were generated and cover the entire tunnel basin area, while in the crown portion, displacements of 0.048 m were observed. At the extremes of the model, settlements of a magnitude of 0.01 m were generated.

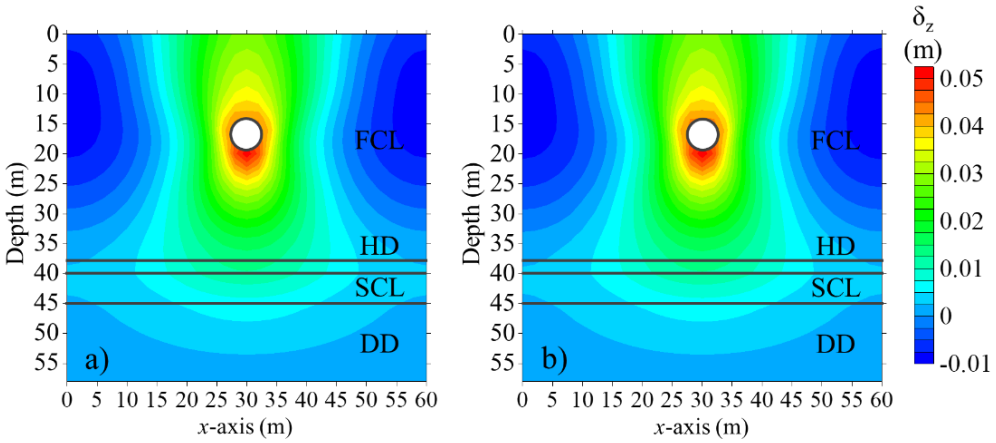


Fig. 16 Cross sections of the expected value of the vertical displacements (1,000 simulations) a) Expected value of vertical displacements (36 soil units in FLC) and b) Expected value of vertical displacements (483 soil units in FLC)

The expected value of the vertical displacement field obtained in the stochastic analysis shows consistency in distribution and magnitude of displacements with the results obtained in the deterministic analysis.

Standard deviation

Figure 17 presents the distribution of the standard deviation of the vertical displacements, considering both the 1D vertical (Fig. 17a) and 3D variabilities (Fig. 17b) of the E_u modulus. Three zones can generally be identified. The highest values of uncertainty in the vertical displacements occurred in a first zone situated in the central portion of the section, where the tunnel is located. These maximum values were found in the basin of the lining. The standard

deviation values presented in Figure 17a around the tunnel are larger than those presented in Figure 17b. This coincides with the larger scattering of the maximum displacement values observed in the convergence analyses. This can be attributed to a statistical compensation effect that leads to less uncertainty in the response of the system in the 3D case of E_u variability (Auvinet et al. 1996).

In a second zone covering the most extensive area of the cross-sections, in which the expected value of vertical displacements tends to zero, the standard deviation values are also close to zero. In the third zone, located close to the lateral boundaries of the cross-section, standard deviation values range from 0.0016 m to 0.002 m.

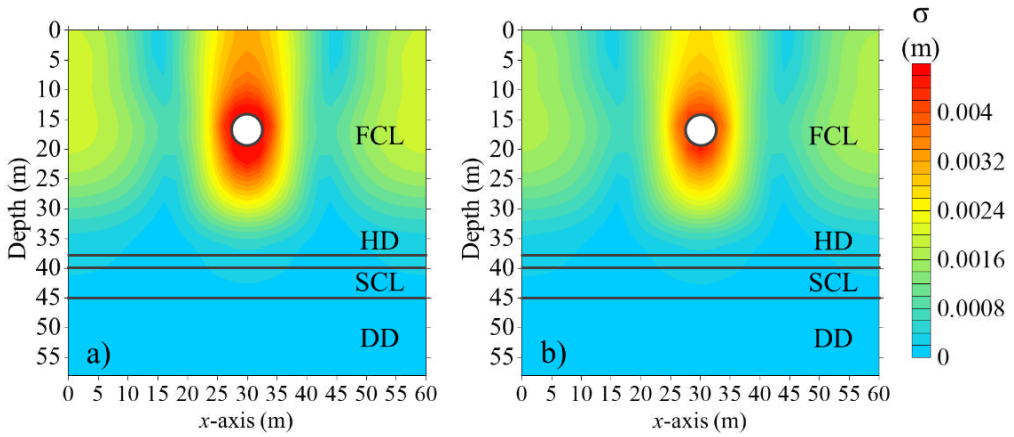


Fig. 17 Cross sections of standard deviation of vertical displacements (1,000 simulations) a) Standard deviation of vertical displacements (36 soil units in FLC) and b) Standard deviation of vertical displacements (483 soil units in FLC)

Coefficient of variation of vertical displacements

Figure 18 presents cross-sections of the coefficient of variation (*CV*) of the vertical displacements of the tunnel. Figures 18a and 18b illustrate the distribution of *CV* values across both sections. Again, three distinct zones were clearly defined. The first zone corresponds to the central region of the tunnel section, where the *CV* ranges from 0 to 20%. The highest *CV* values (20%) in this zone were found near the lining. This is congruent with the region in which the maximum upward displacements of the tunnel are observed.

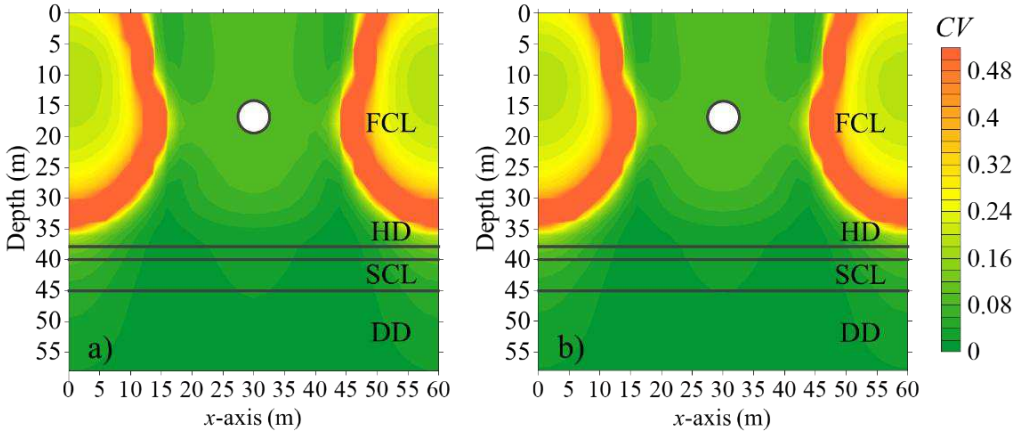


Fig. 18 Cross section of coefficient of variation of vertical displacements (1,000 simulations, a) Coefficient of variation of vertical displacements (36 soil units in FLC) and b) Coefficient of variation of vertical displacements (483 soil units in FLC)

The second zone demonstrates the highest *CV* values across the entire cross-section, exceeding 40%, and corresponds to the area where expected vertical displacements are close to zero and *CV* can tend to infinity. In this zone, using coefficient of variation *CV* to quantify uncertainty can thus be considered as inadequate. Finally, at the boundaries of the *CV* segments, a region was identified where the variation range is between 20% and 40%, corresponding to the area where downward vertical displacements occur within the soil mass.

In this application, the cross-sections of the coefficient of variation, in addition to quantifying the uncertainty in vertical displacements, allows defining the boundary where change in the direction of the displacements (upward, downward) occurs.

6 Conclusions

Deterministic analyses and field observations show that tunnels in soft soils present an upward displacement during the excavation process and installation of the primary lining. This is known as the 'bubble effect', a phenomenon which is especially conspicuous in highly deformable soils, such as those found in the Valley of Mexico.

In this paper, the uncertainty on short-term vertical displacements of tunnels in soft ground, considering the spatial variability of the undrained elastic modulus (E_u) of the soil was assessed.

The spatial variability of the soil was represented by random fields. Analysis of the available geotechnical data revealed that the modulus (E_u) field in the first clay layer (FCL) exhibits a highly anisotropic correlation structure. The horizontal correlation distance is considerably larger than the vertical one. This condition is associated with the lacustrine soil formation process of Mexico City clays. A simplified 1D model and a 3D random field model were employed to represent this condition.

The incorporation of the variability of the E_u modulus into the numerical analysis was performed dividing the stratigraphy into soil units and assigning simulated values of this parameter to each soil unit. The dimensions of the soil units were chosen as clearly smaller than the correlation distance of the parameter.

The uncertainty analysis was performed using the stochastic finite element method. Monte Carlo simulations were used to represent different scenarios considering the variability of E_u modulus. The uncertainty on vertical displacements was estimated calculating the displacement standard deviation. The maximum uncertainty value on displacement was found in the tunnel basin area, where the greatest upward displacements. In this case, using the coefficient of variation of displacement to quantify uncertainty was found to be inadequate, since this parameter tends to infinity at the boundaries between zones of downward and upward vertical displacements (settlements and heaves), where the expected displacement value is close to zero.

The stochastic analyses presented indicate that when considering the vertical 1D variability of the undrained elastic modulus, the uncertainty on the displacements is slightly higher than in the case of the three-dimensional random field. This can be attributed to the statistical compensation effect mentioned by Auvinet et al. (1996). However, it can be considered that a 1D model can give acceptable results for materials with a highly anisotropic correlation structure such as Mexico City clays.

Statements and declarations
All authors declare that they have no conflicts of interest.

Acknowledgments
The authors thank the anonymous reviewers for their comments and suggestions, which improved the present analysis manifold.

Funding
This research was funded by Geoinformatics group, Institute of Engineering of UNAM, and Secihti (Secretaría de Ciencia, Humanidades, Tecnología e Innovación).

References

Ali A, Lyamin A, Huang J, Sloan S, Cassidy M (2017) Undrained stability of a single circular tunnel in spatially variable soil subjected to surcharge loading. Computers and Geotechnics. (84) 17-24 https://doi.org/10.1016/j.compgeo.2016.11.013

Alabert F (1987) The Practice of Fast Conditional Simulations Through the *LU* Decomposition of the Covariance Matrix. Mathematical Geology, Vol. 19, No. 5. https://doi.org/10.1007/BF00897191

Auvinet G (2002) Uncertainty in Geotechnical Engineering, 16th Nabor Carrillo Lecture, Sociedad Mexicana de Mecánica de Suelos, Mexico

Auvinet G (2019) Geotechnical Engineering in Spatially Variable Soft Soils. The Case of Mexico City. The 9th A. Casagrande Lecture. https://doi.org/10.3233/ASMGE190004
Auvinet G (2025) Procesos estocásticos y Campos aleatorios (Stochastic processes and random fields). Publication of Instituto de Ingeniería, UNAM, Mexico
Auvinet G, Abaziou L (1993) Application of random field theory to control of compaction of earth embankments, Sciences de la Terre, N° 32, 449-460, Nancy, France
Auvinet G, Bouayed A, Orlandi S, López A (1996) Stochastic Finite Element Method in Geomechanics, ASCE GSP N° 58, Vol. 2, 1239-1253, ISBN 0-7844-0188-8, USA
Auvinet G, Méndez E, Juárez M (2017) El subsuelo de la Ciudad de México. Vol 3. Instituto de Ingeniería, UNAM. CDMX, Mexico
Auvinet G, Rodríguez J (2011) Analysis, design, construction and behavior of underground structures in soils. Proceedings, XIVth Pan-American Conference on Soil Mechanics and Geotechnical Engineering, Vol. 1 pp. 377-385, Toronto, Canada
Baecher G (2023) 2021 Terzaghi Lecture: Geotechnical systems, uncertainty, and risk. Journal of Geotechnical and. Geoenvironmental Engineering. 149 (3). https://doi.org/10.1061/JGGEFK.GTENG-10201
Bobet A, Einstein H (2023). Tunnel Design Methods (1st ed.). CRC Press
Chilès J, Delfiner P (1999) Geostatistics: Modeling Spatial Uncertainty. Wiley, New York. https://doi.org/10.1002/9780470316993
Ching J, Hu Y (2016) Effect of element size in random finite element analysis for effective young's modulus. Mathematical Problems in Engineering. https://doi.org/10.1155/2016/8756271
Christian J (2004) Geotechnical engineering reliability: How well do we know what we are doing? Journal of Geotechnical and. Geoenvironmental Engineering. 130 (10). https://doi.org/10.1061/(ASCE)1090-0241(2004)130:10(985)
Crisp M (2020) The optimization of geotechnical site investigations for pile designing multiple layer soil profiles using a risk-based approach, Ph.D Dissertation, Adelaide: University of Adelaide
Crisp M, Banks C, Shivasami A, Davies O (2022) The Random Finite Element Method, Its Implementation in Geotechnical Software Through Python, and a Comparison with the Random Limit Equilibrium Method. Geotechnical Lessons Learnt—Building and Transport Infrastructure Projects. Sydney Symposium. Lecture Notes in Civil Engineering, vol 541. Springer, Singapore
Davis M, (1987) Production of Conditional Simulations via the LU Triangular Decomposition of the Covariance Matrix. Mathematical Geology 19, 91–98. https://doi.org/10.1007/BF00898189
El-Ramly H, Morgenstern N, Cruden D (2002) Probabilistic slope stability analysis for practice. Canadian Geotechnical Journal.39(3).https://doi.org/10.1139/t02-034
Feng C, Zheng Z, Beer M (2025) Efficient simulation of conditional random fields and its geotechnical applications, Engineering Geology. 356, 1-17. https://doi.org/10.1016/j.enggeo.2025.108284
Fenton G, Griffiths V (2008) Risk assessment in geotechnical engineering. Wiley, New York. http://dx.doi.org/10.1002/9780470284704
Ghanem R, Spanos P (1991) Stochastic Finite Elements: A Spectral Approach, Springer-Verlag, Berlin, second edition, Dover Publications, NY. https://doi.org/10.1007/978-1-4612-3094-6
Griffiths D, Fenton G (2007) Probabilistic Methods in Geotechnical Engineering. Springer, Berlin. https://doi.org/10.1007/978-3-211-73366-0
Gong W, Juang C, Martin J, Tang H, Wang Q, Huang H (2018) Probabilistic analysis of tunnel longitudinal performance based upon conditional random field simulation of soil properties. Tunneling and Undergrown Space Technology. 73, 1–14. https://doi.org/10.1016/j.tust.2017.11.026
Huang J, Griffiths D (2015) Determining an appropriate finite element size for modelling the strength of undrained random soils. Computers and Geotechnics, 69, 506–513. https://doi.org/10.1016/j.compgeo.2015.06.020
Huang H, Xiao L, Zhang D, Zhang J (2017) Influence of spatial variability of soil Young's modulus on tunnel convergence in soft soils. Engineering Geology 228, 3. https://doi.org/10.1016/j.enggeo.2017.09.011
Hristopulos D (2020) Random Fields for Spatial Data Modeling: A Primer for Scientists and Engineers. Springer Nature. https://doi.org/10.1007/978-94-024-1918-4
Li P, Liu S, Ji J, Ding X, Bao M (2023) Stochastic analysis of excavation-induced wall deflection and box culvert settlement considering spatial variability of soil stiffness Journal of Rock Mechanics and Geotechnical Engineering, 15(12). https://doi.org/10.1016/j.jrmge.2023.02.024
Li X, Wu Z, Su D, Zhang L (2024) Reliability analysis of offshore monopile foundations considering multidirectional loading and soil spatial variability. Computers and Geotechnics. 166, 106045. https://doi.org/10.1016/j.compgeo.2023.106045

Liu H, Chen X, Cheng P, Hu Y (2025) An efficient approach for determination of equivalent design strength and probability of failure for tunnel face in spatially random soils. Journal of Structures, 73, 108346. https://doi.org/10.1016/j.istruc.2025.108346

Papadopoulos V, Giovanis D (2018) Stochastic Finite Element Methods: An Introduction, Mathematical Engineering, Springer International Publishing AG. https://doi.org/10.1007/978-3-319-64528-5

Peck R (1969) State of the Art Report. Deep Excavation and Tunneling in Soft Ground. Proceedings 7th International Conference on Soil Mechanics and Foundation Engineering, State-of-the-Art Volume, Mexico City, Mexico. Sociedad Mexicana de Mecánica de Suelos, pp. 225–290

Penning R, dos Santos B, Palomino J, Quiroz K (2025) Use of random fields in slope stability analysis and application to a case history. Journal of the Brazilian Society of Mechanical Sciences and Engineering 47 (290). https://doi.org/10.1007/s40430-025-05601-1

Phoon K (2023) What geotechnical engineers want to know about reliability. ASCE-ASME Journal of Risk and Uncertainty in Engineering Systems, Part A: Civil Engineering 9 (2). https://doi.org/10.1061/AJRUA6.RUENG-1002

Phoon K, Kulhawy F (1999) Characterization of geotechnical variability. Canadian Geotechnical Journal.36(4): 612-624. Characterization of geotechnical variability. https://doi.org/10.1139/t99-038

Popescu R, Prevost H, Deodatis G (1997) Effects of spatial variability on soil liquefaction: Some design recommendations. Geotechnique. 47 (5), 1019–1036. https://doi.org/10.1680/geot.1997.47.5.1019

Popescu R, Deodatis G, Nobahar A (2005) Effects of random heterogeneity of soil properties on bearing capacity. Probabilistic Engineering Mechanics,20 (4),https://doi.org/10.1016/j.probengmech.2005.06.003

Rodríguez J, Santos E, Auvinet G (2024) Three-dimensional numerical simulation of tunneling in soft soils with TBM-EPB. XVII Pan-American Conference on Soil Mechanics and Geotechnical Engineering (XVII PCSMGE).

Serhal R, Peña-Olarte A, Miraei M, Schoor J, Wiegel A (2025) Deterministic versus random finite element analysis of tunnel response: a case study in Munich area. Geotechnical and Geological Engineering 44, 14. https://doi.org/10.1007/s10706-025-03512-5

Stefanou G (2009) The stochastic finite element method: Past, present and future. Computer Methods Applied Mechanics and Engineering. https://doi.org/10.1016/j.cma.2008.11.007

Vanmarcke E (1977) Probabilistic modeling of soil profiles. Journal of the Geotechnical Engineering Division, ASCE, 103(GT11): 1227–1245. https://doi.org/10.1061/AJGEB6.0000517

Vanmarcke E (1984) Random fields, analysis and synthesis. MIT Press, Cambridge, Mass.

Wu Y, Bao H, Wang J, Gao Y (2021) Probabilistic analysis of tunnel convergence on spatially variable soil: The importance of distribution type of soil properties, Tunneling and Underground Space Technology, 109. https://doi.org/10.1016/j.tust.2020.103747

Xie D, Su H, Fang Z (2025) A Reliability Analysis Approach for Embankment Stability Considering Spatial Variability of Soil Properties. International Journal for Numerical and Analytical Methods in Geomechanics. https://doi.org/10.1002/nag.70148

Zaldivar F, Rodríguez J, Auvinet G (2012) Esfuerzos y desplazamientos alrededor de un túnel considerando el "efecto burbuja", 2° Simposio Internacional sobre túneles y lumbreras, SMIG, AMITOS, México.

Zheng Z, Dai H, Beer M (2023) Efficient structural reliability analysis via a weak-intrusive stochastic finite element method. Probabilistic Engineering Mechanics, 103414. https://doi.org/10.1016/j.probengmech.2023.103414

Zhou Z, Li X, Zhao H (2022) Probabilistic Study of Offshore Monopile Foundations Considering Soil Spatial Variability. ASCE-ASME Journal of Risk and Uncertainty in Engineering Systems, Part A: Civil Engineering, 8(4). https://doi.org/10.1061/AJRUA6.0001259